Biosensors and Bioelectronics 130 (2019) 374–381

Contents lists available at ScienceDirect

Biosensors and Bioelectronics

journal homepage: www.elsevier.com/locate/bios

Hybrid electrochemical sensor platform for capsaicin determination using coarsely stepped cyclic squarewave voltammetry

Sindre Søpstad*, Kristin Imenes, Erik A. Johannessen

Department of Microsystems, Faculty of Technology, Maritime and Natural Sciences, University of South-Eastern Norway, Borre, Norway

ARTICLE INFO

Keywords:
Capsaicin
Electrochemical biosensors
Hybrid electronics
Chili hotness
Screen-printed electrodes

ABSTRACT

A small, standalone electrochemical hybrid sensor platform, combining flexible electronics and screen-printed electrodes, is demonstrated in the determination of capsaicin through adsorptive stripping voltammetry. The sensing scheme was simplified to be compatible with a low-cost device. The simplification involved eliminating the need for additional modification of the electrode and employing a coarsely stepped squarewave voltammetry, a technique which is applicable with less sophisticated instrumentation. This architecture was found to be suitable for concentrations up to at least 5000 μM with a detection limit of 1.98 μM. The screen-printed carbon graphite electrodes were made reusable through an ethanol rinsing protocol. The effect of ethanol/buffer volumetric ratio in the test sample was shown to greatly influence the analytical data, and a fixed 10% (v/v) was chosen as a compromise between signal-to-noise ratio and not exceeding the solubility limit of the desired upper range.

1. Introduction

Capsaicinoids are the chemical compounds responsible for most of the pungency or "hotness" associated with the Capsicum family of plants. The more potent species such as chilies are one of the most popular food additives (Barbero et al., 2008). Capsaicin, the most abundant capsaicinoid, is known for the many positive effects it has on the human health, such as antimutagenic, anticarcinogenic, anti-inflammatory and antitumoral properties (Fattori et al., 2016). It has also been shown to have combative effects on back pains, cholesterol, obesity and gastric ulcv (Satyanarayana, 2006). Additionally, it is found in pharmaceutical products such as pain relief dermal patches, ointments and creams. Capsaicin is the active ingredient in weapons used for riot control and pepper spray used for self-defense (Yard and Zühre, 2013). Hence, its use would benefit from an accurate and cheap method for quantifying its content.

The hotness of the plant is traditionally measured organoleptically in units of Scoville Heat Units (SHU), and stems from the process of a panel of humans tasting samples at different levels of dilution until the hotness could no longer be tasted (Scoville, 1912). This process is undoubtedly labor intensive and prone to subjective interpretation. In molar quantities the capsaicin may range from sub-nM to, in extreme cases, several hundred mM. The dynamic range is therefore an important performance parameter for an analytical assay in order to limit extensive dilution processes (Randviir et al., 2013a, 2013b).

Electrochemical detection of capsaicin content has therefore been investigated as a cost-effective and simple alternative to more complex techniques, such as high-performance liquid chromatography (HPLC). Enzyme mediated assays have proven to work well with simple techniques such as chronoamperometry in applications like glucose monitoring for diabetes management (Wang, 2001), and there has been some recent development for enzymatic capsaicin sensors (Mohammad et al., 2017, 2013). However, if the biocatalyst can be omitted from the sensor, design considerations related to an added manufacturing process step and enzyme degradation can be disregarded. The sensing scheme for the label-free electrochemical detection of capsaicin was initially proposed by the Compton group (Kachoosangi et al., 2008). They utilized that capsaicin adsorbs to carbon surfaces. By stimulating the adsorbed capsaicin through cyclic voltammetry (CV), also known as adsorptive stripping voltammetry (AdSV), they put it through an $EC_{irr}EE$ reaction scheme. The resulting voltammogram fingerprints the molecule, and the peak currents (or charge) may be used for quantitative analysis. The process is outlined in Scheme 1. Two cycles are needed, where upon the first ramp, electrooxidation (E) of capsaicin takes place (peak I). This is immediately followed by an irreversible hydrolysis step (C_{irr}) which transforms the phenolic group in the structure of capsaicin into a σ-benzenoquone, and thusly makes up the oxidized form of the well-known catechol redox couple (Manaia et al.,

* Corresponding author.
E-mail address: sso@usn.no (S. Søpstad).

https://doi.org/10.1016/j.bios.2018.09.036
Received 28 June 2018; Received in revised form 29 August 2018; Accepted 12 September 2018
Available online 14 September 2018
0956-5663/

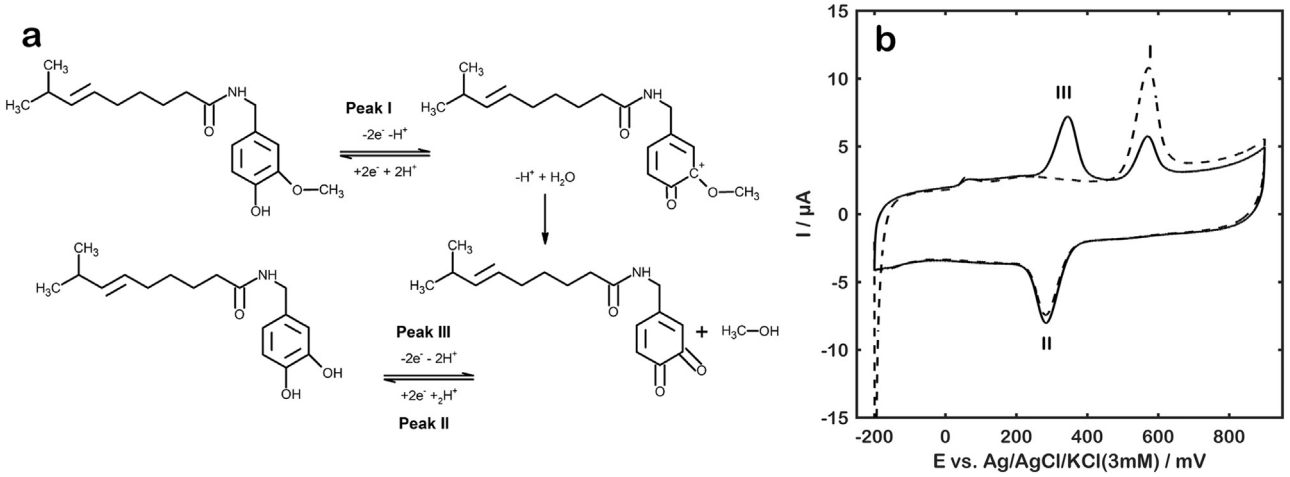

Scheme 1. Adsorptive stripping voltammetry (a) reaction pathway, and (b) voltammograms for the first (–) and second (-) scan.

2012). This redox cycle (EE) takes place at peaks II and III. Using a screen-printed carbon electrode modified with multiwalled carbon nanotubes (MWCNT-SPEs), capsaicin could be determined up to at least 35 µM with a lower limit of detection (LOD) of 0.45 µM (Kachoosangi et al., 2008).

Since this discovery, succeeding literature has focused on expanding the measurable range, with emphasis on lowering the LOD. In general, this has been achieved through a more complex modification of the electrode. One exception to this is Ruas de Souza et al., who achieved a ~2x sensitivity gain simply by mirroring a screen-printed electrode (SPE) onto the "dead-space" on its backside, essentially having two sensors on the same footprint (Ruas de Souza et al., 2015), resulting in LOD of 0.18 µM. The limitation of this architecture is that the whole sensor has to be submerged into the test solution (as opposed to dropping small sample volume onto a horizontally oriented, single-sided sensor), requiring higher sample volume, or added liquid handling. Baytak & Aslanoglu developed a sensor to specifically target lower concentrations (0.01–0.41 µM) by modifying carbon nanotubes with Ru nanoparticles and applying them a to glassy carbon electrode (Kutluay and Aslanoglu, 2017). Electrochemical impedance spectroscopy was utilized to measure more concentrated capsaicin (up to 4000 µM) with an LOD of 220 µM on screen-printed carbon electrodes modified with CNTs, avoiding the dilution steps required by the original scheme (Randviir et al., 2013a, 2013b). This was believed to be impossible with CV due to the oxidation peaks merging and shifting outside the potential window of interest, although CV was still found to be the best technique at lower concentrations. EIS however, requires quite complex instrumentation, involving a precise signal generator, phase analyzer etc., which is harder to implement in a simple, low-cost device.

The development of a low cost capsaicin detection system would need to share some common traits with existing electrochemical sensors. Many of these are based on screen-printing, which is a scalable and low cost technique for patterning metals and other materials on almost any surface. Thus far, the greatest success story of screen-printed biosensors is that of glucose test strips for diabetes monitoring (Turner, 2013). Flexible electronics has gained considerable attention in the biosensing field due to its many advantages, while benefiting from the scalability, complexity and low cost of the mature rigid printed circuit boards (PCBs). Among its advantages are conformity and light weight. Combining screen-printing with flexible electronics (hybrid technology) may prove a powerful tool in providing conformable, light-weight, and low-cost sensing platforms. The applications range from food safety (both in manufacturing and during storage) and health tracking, to pharmaceuticals manufacturing and environmental monitoring in inaccessible locations such as corrosion monitoring in concrete structures (Abbas et al., 2013; Duffó et al., 2010; Jin et al., 2016), sensors deployed by drones, or pollution monitoring in oceans and lakes.

In this work we present a simplified method for capsaicin detection using unmodified SPEs and coarsely stepped cyclic SWV (CCSWV). This simplification in fabrication and measurement technique allows for better suitability in low-cost sensor platforms while still having the greatest reported range of capsaicin detection for a single technique. Furthermore, we demonstrate a standalone electrochemical detection platform capable of performing this task.

2. Experimental section

2.1. Reagents and apparatus

Britton-Robinson (BR) buffer pH 2 and capsaicin stock solution, 0.05 M in ethanol, was acquired from Aliksir Ltd. All other chemicals were purchased from Sigma-Aldrich and were of reagent grade purity. Test solutions with certain capsaicin concentrations were prepared freshly each day. Voltammetric measurements were conducted with a potentiostat (Ana Pot) and screen-printed carbon graphite electrodes (SPREs, A-AC-CAC-203-N), both acquired from Zimmer & Peacock AS. In the case of coarsely stepped SWV, no raw data filtering was employed, as the spiky nature of the peaks would be recognized as anomalies and sought corrected. For CV, a Savitzky-Golay spike rejection filtering was implemented to smooth out any anomalous spikes. 3 mM KCl was added to the test samples in order to have the screen-printed reference electrodes (Ag/AgCl) to be operating at a known potential (370 mV vs. SHE), while keeping the analytical signal within the potential window of the device.

2.2. Analytical procedures

A 50 µL aliquot of sample solution containing different concentrations of capsaicin was dispensed onto the electrodes. The effect of accumulation time has been explored previously (Kachoosangi et al., 2008; Randviir et al., 2013a, 2013b; Wang et al., 2016; Yard and Zühre, 2013). In general, a higher accumulation time will allow more matter to adsorb to the surface, giving a higher analytical signal and possibly a lower detection limit. On the other hand, the surface will reach maximum coverage at a lower concentration, limiting the sensor's upper detection range. An accumulation time of 60 s at open-circuit potential was chosen for our application. This time was chosen as it provides a convenient mid-point between adsorbing enough analyte to allow detection at lower concentrations, while retaining a high upper detection limit by preventing early surface saturation, and at the same time keeping the protocol execution time down. The open circuit-potential was monitored during this step in an effort to gain additional

information about the state of the system without perturbing it. Following the accumulation time, the two cycles of CV or CCSWV was performed. For CV the electrodes were scanned between −200 mV and + 900 mV vs. Ag/AgCl/KCl(3 mM). For CCSWV the electrodes were scanned between −240 mV and + 720 mV with a 60 mV step size and 60 mV amplitude at 3 Hz, resulting in an effective scan rate of 240 mV s^{-1}.

The effect of pH has been thoroughly investigated in the literature (Ang et al., 2017; Kachoosangi et al., 2008; Wang et al., 2016; Ya et al., 2012a; Yardım, 2011). The reaction scheme has been established to be pH dependent, and the reaction pathway is the same in the range pH 1–9. The voltammogram maintains its shape in this range but has a nernstian potential shift along the voltage axis, as well as a reduced signal strength, with increasing pH. The importance therefore lies in maintaining the pH constant, i.e. buffering the sample to reduce the variability, and keeping the pH low for enhanced sensitivity. The acquired buffer was therefore used as received (pH 2) without adjusting the pH.

2.3. Circuit design

A standalone electrochemical sensor platform with a material cost of about ~ 25 € was developed in order to realize a low-cost capsaicinmeter (Fig. 1). Schematic design and bill of materials can be found in the Supplementary material. Although it is being demonstrated for capsaicin detection in this paper, it is intended to be generic platform that permit the use of multiple electrochemical techniques, such as amperometry, coarse voltammetry and open-circuit potentiometry, and can be operated both in continuous and one-shot mode. It is schematically inspired by two application notes from Texas Instruments and Johanson Technology (Johanson Technology, 2012; Singh, 2013), and has been modified into a 4-layer flexible printed circuit board populated with the following main components: A microcontroller (CC2541, Texas Instruments) with built-in Bluetooth low energy (BLE) and analog-to-digital converters was utilized for circuit control, data conversion and wireless data transfer (Fig. 1b v-vi). A boost-converter chip (TPS61220, Texas Instruments, Fig. 1b iii) was employed to regulate the voltage delivered from the flexible thin-film battery (BV-452229-17ET, Brightvolt LLC). Two analog-front end circuits were used for sensor-readout and conditioning. A chip potentiostat (LMP91000, Texas Instruments, Fig. 1b ii) was utilized for voltammetric and amperometric capability, and a unity-gain instrumentation amplifier (MAX4461, Maxim Integrated) for open circuit potentiometric measurements (not used here). Working, reference and counter electrodes were screen-printed directly onto the PCB. The PCB was designed through KiCad EDA (Ver. 2017-07-13, KiCad developers), and manufactured out-of-house (Flexible PCBs, PCBway). The electrodes are placed on their own peninsula (Fig. 1b i) to limit splash damage to the electronic components, and to allow free movement of the sensor head, such that it might conform to the individual application's requirements. For wearable applications it would be convenient to fold the electrodes such that they are in contact with the skin, while the electronic components are not. For microlitre drop testing the sample would be pipetted directly onto the electrodes. On the end opposing the electrodes, there is a second peninsula holding pinouts for programming and debugging (Fig. 1b vii). Among the debugging functionality is the breakout of the electrodes, so they can be addressed by different instrumentation, effectively bypassing the on-board electronics if required. This is designed such that it can be cut off before deployment to further limit the size of the device. A mold was 3D-printed (Lulzbot TAZ 6, Aleph Products Inc.) to allow encapsulation of the circuit. The mold, depicted in Fig. 1c, is a hollow block with openings for both peninsulae (Fig. 1d). Conformal silicone coating (3140, Dow Corning Co.) or thermoplastic glue, was poured over the circuit and allowed to cure, forming a water repellant seal around the part of the device holding the electronic components (Fig. 1e).

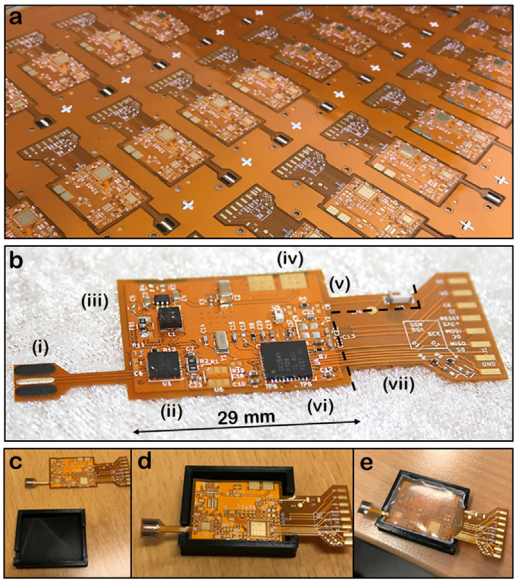

Fig. 1. Photograph of electrochemical sensor platform (a) on a 25 × 25" panel before component assembly and (b) single sensor platform after assembly. The roman numerals indicate (i) the screen-printed electrodes, (ii) chip potentiostat, (iii) battery management circuitry, (iv) terminals for flexible battery (dimensions 29 × 25 × 0.6 mm) situated on the backside, (v) antenna circuitry for Bluetooth low energy, (vi) microcontroller with integrated analog-to-digital converter, and (vii) debug circuitry which can be cut off (–) before deployment. (c-e) Photographs of the encapsulation of the electronics components in a 3D-printed mold.

In this paper we employed the sensor platform in SWV mode and utilized carbon working and counter electrodes (C2000802P2) and a silver/silver-chloride reference electrode (C2130916D4) from Gwent Electronics Manufacturing Ltd. The electrodes were printed with a semi-automatic screen-printer (DEK 248, ASM Assembly Systems) through steel stencils (SMD Stencils, Pcbway) and cured in a box oven for 30 min at 60 °C (Fig. 1a). The electronic components were manually reflow soldered, after which the circuit was programmed through IAR Embedded Workbench 8051 (IAR Systems). The complete circuit is depicted in Fig. 1b.

3. Results and discussion

3.1. Electrode re-usage

It is desirable to be able to re-use the electrodes since they constitute a permanent part of the sensor system that cannot be replaced. Although DI-H_2O previously have been used to rinse the working electrode between measurements (Kachoosangi et al., 2008; Mpanza et al., 2014), it was found that this method left residual peaks (Fig. 2a), indicating that the substances of the reaction scheme are still present on the electrode. This would create a falsely high sensitivity if tested under ascending concentrations of capsaicin and the response would therefore heavily rely on the history of the electrode, a parameter which would be cumbersome to keep track of in a real application. Instead, a solution comprising ethanol (> 50% v/v) and buffer was found to effectively remove the residual peaks, as evidenced by Fig. 2a. First, any residual sample was blown off by compressed air. Ethanol-buffer solution was then trickled across the electrodes for around 5 s, which were held at a ~ 45° angle, using a syringe, followed by evacuating the solution with compressed air. This ritual was repeated a total of three times, consuming about 1 mL of the rinsing solution and 45 s of time.

A side effect of the ethanol rinse is that the baseline signal (non-peak regions) is amplified. This was remedied by subtracting the baseline signal (no capsaicin) from the signal obtained in the presence

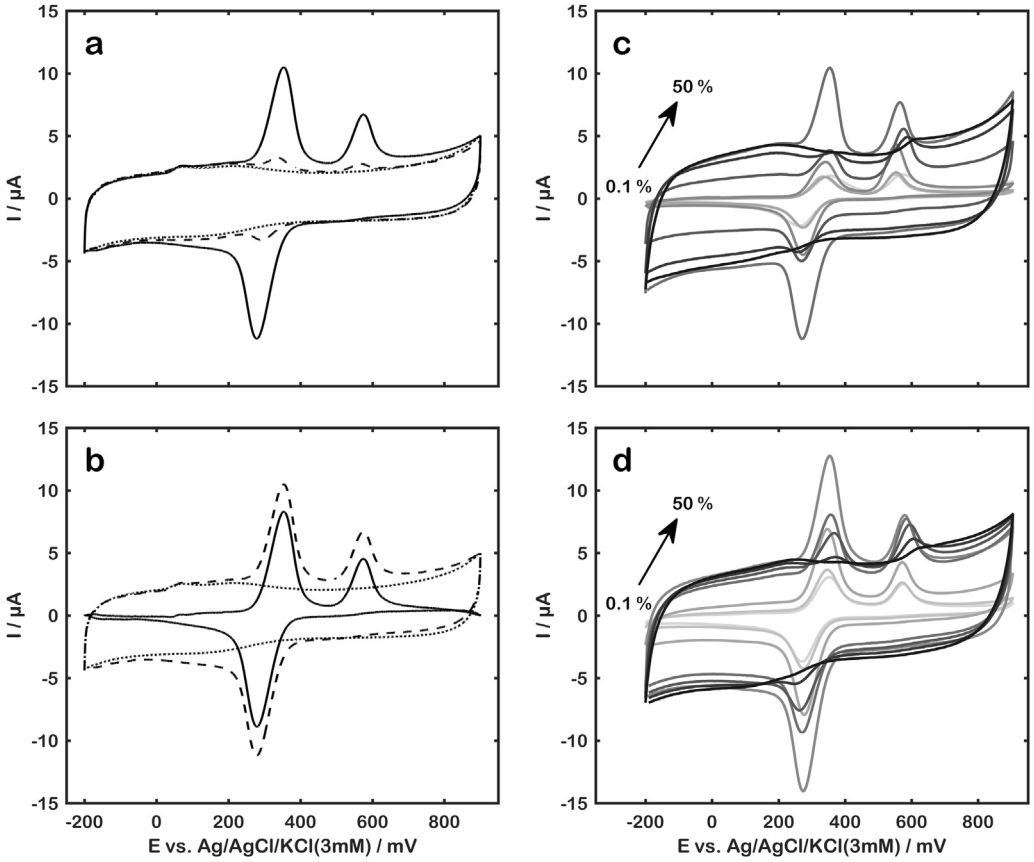

Fig. 2. (a) Cyclic voltammograms (second scan) in the absence of capsaicin after cleaning by DI-H2O (–) or ethanol (··) following a measurement of 50 µM capsaicin (-). (b) Baseline corrected voltammogram (-) obtained through subtracting the baseline (··) from the raw signal (–). (c) The influence of ethanol content (% v/v) at a fixed 50 µM capsaicin concentration for fresh and (d) reused electrodes. The ethanol content increases as the shade of the traces darken.

of capsaicin, as demonstrated in (Fig. 2b). This allowed for easier peak detection, since peaks II and III would originally ride on a shoulder of the blank at lower concentrations.

3.2. Ethanol content

Since the capsaicin stock solution had ethanol as the solvent, making up different concentrations in pure buffer solution would consequently change the ethanol content. An investigation was carried out to determine the effect of varying ethanol content. Fig. 2(c and d) shows the AdSV (2nd cycle) response of different ethanol content under constant 50 µM capsaicin concentration, for both fresh and re-used electrodes. For both kinds of electrodes, at lower concentrations (0.1–1% v/v), the baseline and analytical signal are low, but the signal to baseline ratio (S/B) is high enough to easily distinguish the analytic peaks from the baseline signal. As the ethanol increases (5–20%), as does the baseline. The peaks ride on-top of this signal, making them easy to spot, especially through the baseline correction described in 3.1. At higher concentrations, the peaks start to retract the into baseline and vanish completely at 50%. Presumably, this is due to capsaicin being hydrophobic, and prefers to adsorb to carbon when the bulk solution contains primarily water. However, when the solution is rich on ethanol, remaining in the bulk provides a lower energy state, and what little capsaicin is adsorbed is masked by the magnified baseline signal that occurs at higher ethanol concentrations. The presumption is backed by that a concentration greater than 50% was needed in order to remove any residual peaks, as discussed in 3.1. A second explanation could be that the ethanol content changes the electrical double layer characteristics in such a way the system becomes primarily capacitive, thus prohibiting charge transfer. Indeed, the voltammograms increasingly take on the quasirectangular profile associated with capacitive behavior. Note that neither of these hypotheses does not preclude the other.

In order not to exceed the solubility limit at the highest concentration investigated (5000 µM), and at the same time maintain a high S/B-ratio, a 10% v/v ethanol was chosen to carry out the quantitative assay.

3.3. Cyclic voltammetry on unmodified carbon electrodes

The voltammogram in Fig. 3 shows the electrochemical response of capsaicin through adsorptive stripping voltammetry for a reused unmodified carbon graphite electrode. A linear region was observed in the range 0.5–100 µM for the second ($I_{II}/\mu A = -0.0217\ \mu A\ \mu M^{-1} - 0.0004$, N = 11, $R^2 = 0.993$) and third peak ($I_{III}/\mu A = 0.0159\ \mu A\ \mu M^{-1} + 0.0650$, N = 24, $R^2 = 0.990$). Their corresponding limits of detection (based on 3σ) were estimated to 0.92 µM and 0.48 µM, and their RSD at a fixed concentration of 10 µM was estimated to 3.7% and 4.8% (N = 10). This performance is in line with that reported for single- and multiwalled CNT modified carbon electrodes (Kachoosangi et al., 2008; Randviir et al., 2013a, 2013b). Contrary to these reports, these results suggest that the LOD does not necessarily benefit from employing CNTs, and neither does peak I and III completely merge when passing the 1000 µM mark, as shown in Fig. 3b.

The data was fitted to linearized forms of nine different adsorption isotherm equations: Linear, Langmuir, Freundlich, Dubinin-Radushkevich (D-R), Temkin, Frumkin, Harkins-Jura, Hasley, Henderson (Başar, 2006). The linearized adsorption isotherm fits are provided in the Supplementary material. The ones providing the best regression coefficients ($R^2 > 0.9$) were the Langmuir, Freundlich, Hasley, D-R and Henderson. The Freundlich isotherm (log-log plot) was chosen to represent the calibration data as it provides the simplest mathematical treatment (one operation) of the top five fits ($\log I_{III} = -0.032 \times \log[\text{Capsaicin}] - 8.710$, N = 18, $R^2 = 0.966$). We attribute the deviation from this model at higher concentrations (≥ 1000 µM) to peak I moving outside the potential window and hence not oxidizing all of the adsorbed capsaicin. However, through baseline subtraction and

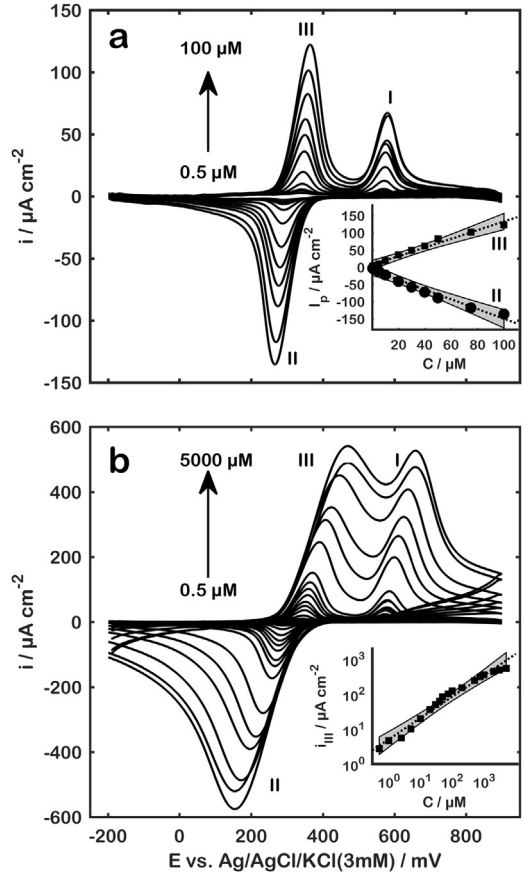

Fig. 3. Baseline subtracted cyclic voltammograms (second scan, 100 mV s^{-1}) for capsaicin concentrations of (a) 0.5–100 µM and (b) 0.5–5000 µM on unmodified carbon graphite electrodes. Insets: calibration plots for the peak currents of the second (II) and/or third peaks (III), where the shaded reagions represent a confidence interval of 99.9%.

an adsorption model, we are able to maintain the LOD while expanding the useable upper range, while eliminating the CTNs from the original ink formulation.

3.4. Coarsely-stepped cyclic squarewave voltammetry

SWV was implemented on the hybrid sensor platform by cycling through the chip potentiostat's available bias voltage steps, which are programmable from −24 to + 24% of the supply voltage (3.0 V) in steps of 2%, i.e. 60 mV. Therefore, the highest precision waveform that could be generated was a square wave amplitude (E_{amp}) of 60 mV and step height of 60 mV (E_{step}), as depicted in Fig. 4a. Cruz et al. demonstrated that the LMP91000 could be used for staircase voltammetry (Cruz et al., 2014). This is, to the best of our knowledge, the first time it has been used for SWV, let alone CSWV. The current was sampled immediately before each voltage step to minimize capacitive contribution, and then transmitted to a smart phone or computer via Bluetooth, allowing for real-time data visualization. To maintain the continuous pulsing, the reversal potential was reused as the first datapoint on the reverse scan. The waveform was validated by connecting a 4.5 kΩ between the WE and CE/RE terminals, and comparing the current-resistance product with a simulated waveform. Good agreement was found through linear regression ($I_R \times R = 0.978$ E mV + 10.709 mV, N = 60, $R^2 = 1.000$).

Capsaicin calibration using CCSWV was carried out with commercially sourced electrodes and potentiostat, and with the developed low-cost sensor platform and integrated electrodes. Their responses are compared in Fig. 4c and d. A linear region was identified in the range 0.5–50 µM for the second and third peaks. The LODs for the second peak were estimated to 0.81 µM ($i_{II}/\mu A\,cm^{-2} = -5.313\,\mu M^{-1} - 1.204$, N = 8, $R^2 = 0.999$) and 1.98 µM ($i_{II}/\mu A\,cm^{-2} = -4.963\,\mu M^{-1} - 72.03$, N = 8, $R^2 = 0.931$) for commercial electrodes and sensor platform, respectively. The LODs for the third peak were respectively estimated to 2.51 µM ($i_{III}/\mu A\,cm^{-2} = 3.109\,\mu M^{-1} + 4.288$, N = 8, $R^2 = 0.992$) and 3.54 µM ($i_{III}/\mu A\,cm^{-2} = -4.963\,\mu A\,cm^{-2}\,\mu M^{-1} - 72.03$, N = 8, $R^2 = 0.9845$). For the commercial electrodes, a RSD at a fixed concentration of 10 µM was estimated to 4.1% and 4.7% (N = 10) for peaks II and III, while for the sensor platform they were estimated to 9.2% and 10.0% (N = 10). The slightly worse performance specs for the sensor platform could be attributed to the resolution of the analog-to-digital conversion. At 12-bit resolution and a current range spanning ± 214 µA, the circuit is only able to discriminate between 104 nA currents at 3.0 V supply voltage. Even so, they are within one order of magnitude of the original report (Kachoosangi et al., 2008).

Due to the limited potential range available with the sensor platform (± 720 mV), the shifting of the peak potentials with concentration caused the signals to plateau at an earlier time. The saturation is likely caused by the peak I during the first scan not being able to oxidize all of the adsorbed capsaicin before the potential is reversed, creating a proportional lowering of peaks II and III, and hence making them indistinguishable from the lower concentrations. Another interesting observation is that for these signals, the height of peak I becomes higher than that of peak III (and II). Furthermore, for these signals, there was an emergence of a peak I′, observed immediately after the potential reversal. All of this combined made possible the criterion for a correction current, i_{corr}, as described by (1), which enabled the use of the entire range investigated. The log-log relationship between i_{corr} and capsaicin concentration can be described by ($\log|i_{corr}/\mu A\,cm^{-2}| = 0.578 \log|\mu M^{-1}| + 1.127$, N = 18, $R^2 = 0.890$) for commercial electrodes and instrument, and ($\log|i_{corr}/\mu A\,cm^{-2}| = 0.390 \log|\mu M^{-1}| + 1.753$, N = 18, $R^2 = 0.981$) for the sensor platform. A higher degree of linearity is reached for the sensor platform, meaning that the corrective current is more effective for this architecture. This is a direct effect of the sensor platform utilizing continuous pulsing through reusing the current sampled at the reversal potential, resulting in a greater *i′*. This is not possible for the commercial potentiostat employed, since CSWV is not part of its repertoire, and must be implemented by stringing together four instances of SWV. In that case, the reversal potential is repeated, and the pulsing becomes discontinuous.

$$i_{corr} = \begin{cases} -i_{II} - i_{I'}, & i_I \geq i_{III} \\ -i_{II}, & otherwise \end{cases} \quad (1)$$

The performance of the sensor platform is compared to other electrode systems in Table 1. While it cannot contend with the lower LOD of the more intricate electrode modifications, its dynamic range is superior, and its LOD is in the same order of magnitude as those modified with carbon nanotubes only.

3.5. Real samples

The device was tested on chili derived sauces available in Norwegian supermarkets. The sauces were diluted in a 1:2 ratio with ethanol and vortexed for > 1 min to ensure good extraction efficiency, and centrifuged (MiniStar, VWR) at 6000 RPM for 5 min. The supernatant was extracted and mixed with the buffer in a 1:9 ratio, leaving the final solution with a 1:19 ratio between sauce and buffer. All measurements were conducted on the same sensor, employing the rinsing scheme in Section 3.1. The following equation was used to convert from concentration to SHU, where *c* refers to the concentration as calculated from (1) and *DF* is the ratio of raw sample to total volume, which in this case was one 20th for all the samples.

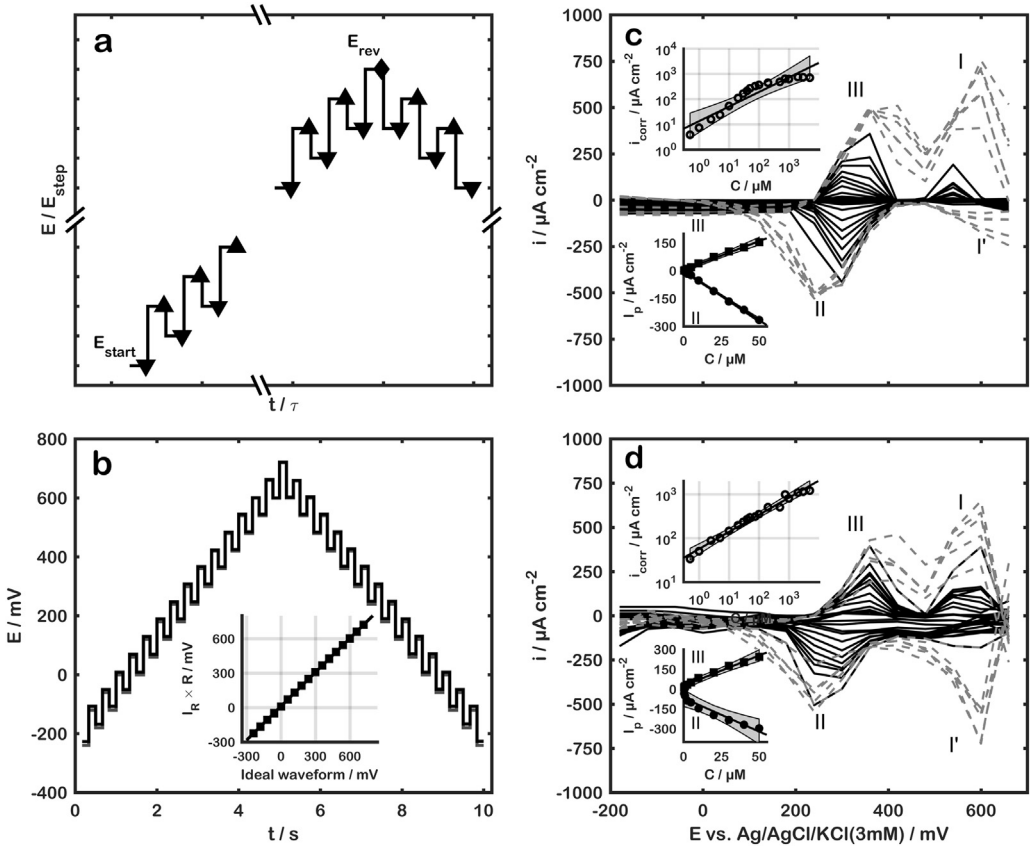

Fig. 4. Voltage waveform for sensor platform showing (a) where the forward (▲), reverse (▼), and the shared reverse/forward (♦) is sampled, and (b) the comparison between a simulated waveform (gray) versus the response of the sensor platform when connected to a 4.5 kΩ resistor (black overlapping the gray). The inset shows the linear regression between the simulated and actual response. (c) Baseline corrected coarse cyclic squarewave voltammograms (second scan) from commercially sourced electrodes and potentiostat, and (d) sensor platform with integrated electrodes and electronics. The dotted lines (–) represent the signals which satisfies $i_I \geq i_{III}$. The top-left insets in the show the corresponding calibration curves from Eq. (1) and the bottom-left insets displays the sensor's linear ranges, where the shaded regions indicate a confidence level of 99.9%.

$$Scoville\ heat\ units = 15\frac{SHU}{ppm}\times 0.3\frac{ppm}{\mu M} \times c\,[\mu M]\times DF^{-1} \quad (2)$$

Tabasco Chipotle, Tabasco Pepper and Tabasco Habanero sauces were estimated to have SHU values of 1612, 4044 and 9578 with RSDs 37.5%, 21.9% and 14.1%, based on triplicate measurements. The calculated values agree well with the SHU ranges supplied by the manufacturer (McIlhenny Company, 2018), of 1500–2500, 2500–500 and > 7000 for the three respective sauces. In contrast to other reports which uses the standard addition method (spiking the samples with different concentrations of synthetic capsaicin) (Kachoosangi et al., 2008; Randviir et al., 2013a, 2013b; Wang et al., 2016; Yard and Zühre, 2013; Yardım, 2011), only one direct measurement is used here, which greatly simplifies the procedure. The results demonstrate that capsaicin determination can be performed by the proposed low-cost, small, reusable, hybrid electrochemical sensor platform.

3.6. Additional considerations

One of the clear weaknesses of electrochemical detection is its susceptibility to interference from other electroactive species in the test matrix, which is especially apparent for label-free assays. It is less of an issue in purified foodstuffs like hot sauces, and pharmaceuticals where the capsaicin content is extremely high compared to other interfering species. However, for testing on the actual peppers, the test matrix becomes much more complex due to the plethora of organic compounds present. Two particularly troublesome substances are ascorbic and ferulic acid, since they are oxidizable within the potential window of the AdSV to detect capsaicin, and commonly present in both plants and foodstuffs. Typically, this creates a broadening of the peaks due to redox peak overlap. This has been elegantly solved by way of transfer voltammetry, or medium exchange voltammetry (Yard and Zühre, 2013): In this procedure, the sensor is exposed to the test matrix for a specific time in order to pre-concentrate (accumulate) the capsaicin on the sensor surface. Due to its strong adsorption, the sensor can be removed from the solution and washed with DI-H_2O or buffer solution, removing most of the unwanted electroactive species that do not strongly adsorb while retaining most of the capsaicin. The sensor is then introduced to a pure buffer solution, enabling the stripping voltammetry to be conducted in a more controlled environment, and with many of the potential interference species removed or greatly reduced. This method increases the potential area of applicability for the proposed platform. Chemicals more closely related to capsaicin, e.g. vanillin or other capsaicinoids are more difficult to deal with and their discrimination in adsorptive stripping voltammetry has yet to be solved, as their voltammograms are hard to discriminate from that of capsaicin. The state-of-the art is therefore to report the total capsaicinoid content rather than any quantification of a single capsaicin derivative (Yard and Zühre, 2013).

Finally, it should be emphasized that this platform is not intended to replace precision laboratory equipment, but rather serve as a bridge for easier deployment of already established and well-known sensor architectures. The fundamental work still needs to be carried out with the best precision available. Only when the sensor has been fully characterized should the decision of being transferred to a low-cost application consisting of a much simpler piece of equipment, like the one presented here, be made.

4. Conclusion

The detection of capsaicin through adsorptive stripping voltammetry on unmodified electrodes was explored for a greater concentration range than previously reported. The lower limit of detection did not suffer significantly from not utilizing carbon nanotubes or other modifying particles in the ink formulation. It was found that deionized water did not completely remove the adsorbed capsaicin derivatives from the electrode surface, and hence, a protocol using ethanol (< 50%

Table 1
Comparison of the performance of different electrode systems.

Electrode system	Adsorption measurement technique	Utilized range / μM	LOD / μM	Reference
Multiwalled carbon nanotube modified basal plane pyrolytic graphite electrode	Cyclic voltammetry	0.5 – 60	0.31	(Kachoosangi et al., 2008)
Multiwalled carbon nanotube modified screen-printed carbon paste electrode	Cyclic voltammetry	0.5 – 35	0.45	(Kachoosangi et al., 2008)
Boron-doped diamond electrode	Squarewave voltammetry	0.5 – 20	0.034	(Yardım, 2011)
Carbon paste electrode modified with amino-functionalized mesoporous silica	Linear sweep voltammetry	0.04 – 4	0.02	(Ya et al., 2012b)
Singlewalled carbon nanotube paste	Cyclic voltammetry	0 – 34	0.77	(Randviir et al., 2013a, 2013b)
Multiwalled carbon nanotube paste	Cyclic voltammetry	0 – 220	1.12	(Randviir et al., 2013a, 2013b)
Multiwalled carbon nanotube paste	Electrochemical impedance spectroscopy	0 – 4 000	220	(Randviir et al., 2013a, 2013b)
Pencil graphite electrode	Squarewave voltammetry	0.016 – 0.32	0.0037	(Yard and Zühre, 2013)
Glassy carbon electrode in ionic liquids	Cyclic voltammetry	0.1 – 10 000	N/A	(Lau et al., 2014)
Glassy carbon electrode modified with gold nanoparticle decorated multiwalled carbon nanotubes	Differential pulse voltammetry	0.15 – 35	0.89	(Mpanza et al., 2014)
Singlewalled carbon nanotube paste in a dual back-to-back electrode configuration	Cyclic voltammetry	5 – 50	0.18	(Ruas de Souza et al., 2015)
Ag/Ag_2O nanoparticle/reduced graphene oxide modified electrode	Differential pulse voltammetry	1 – 60	0.40	(Wang et al., 2016)
Ruthenium nanoparticle modified carbon nanotubes on a glassy carbon electrode	Squarewave voltammetry	0.01 – 0.41	0.0025	(Kutluay and Aslanoglu, 2017)
Screen-printed electrode modified with Poly(Na 4-styrenesulfanate) functionalized graphite	Differential pulse voltammetry	0.3 – 70	0.10	(Ang et al., 2017)
Unmodified carbon graphite electrode	Cyclic voltammetry	0.48 – 5000	0.48	This work
Unmodified carbon graphite electrode	Coarse cyclic squarewave voltammetry	0.81 – 5000	0.81	This work
Hybrid electrochemical sensor platform with unmodified carbon graphite electrodes	Coarse cyclic squarewave voltammetry	1.98 – 5000	1.98	This work

v/v) and buffer solution was instigated. The content of ethanol in the sample solution was found to heavily influence both the baseline signal and the height of the analytical peaks, and was therefore fixed to 10% in order to maximize the detectable range.

The detection scheme was successfully applied to a generic sensor platform, built on a 25 × 29 mm flexible, 1.2 g printed circuit board, with integrated battery, potentiostat and Bluetooth Low Energy communication to a smart phone. The exercise demonstrates that a low-cost, generic electrochemical platform built-from shelf-ware components, is capable of performing the task of more sophisticated laboratory equipment, without significant loss in performance. Future prospects will seek to utilize the same platform for different analytes and other electrochemical measurement techniques.

Acknowledgements

The authors would like to thank the Norwegian Research Council for funding the work presented in this paper, the Norwegian Nanonetworks Ph.D. network for an external fabrication grant (Contract No. 221860/F60), Zimmer and Peacock AS (ZP) and Aliksir Ltd for providing consumables and access to facilities, Dr. Ahn Tuan Nguyen (USN) for advice in the design of flexible electronics, Dr. Thi Thuy Luu (ZP) and Denis Puskar (ZP) for assistance in designing the 3D-printed mold and a custom 3D-printed edge connector for the sensor platform, and Prof. Ulrik Hanke (USN) for inspiring a mechanistic investigation into the sensor response.

Appendix A. Supporting information

Supplementary data associated with this article can be found in the online version at doi:10.1016/j.bios.2018.09.036.

References

Abbas, Y., Olthuis, W., Van Den Berg, A., 2013. A chronopotentiometric approach for measuring chloride ion concentration. Sens Actuators B Chem. 188, 433–439. https://doi.org/10.1016/j.snb.2013.07.046.

Ang, Y.W., Uang, B.H., Ai, W.D., Bin, X.U., 2017. Sensitive electrochemical capsaicin sensor based on a screen printed electrode modified with poly (sodium 4-styrenesulfonate) functionalized graphite. Anal. Sci. 33, 793–799.

Barbero, G.F., Liazid, A., Palma, M., Barroso, C.G., 2008. Fast determination of capsaicinoids from peppers by high-performance liquid chromatography using a reversed phase monolithic column. Food Chem. 107, 1276–1282. https://doi.org/10.1016/j.foodchem.2007.06.065.

Başar, C.A., 2006. Applicability of the various adsorption models of three dyes adsorption onto activated carbon prepared waste apricot. J. Hazard. Mater. 135, 232–241. https://doi.org/10.1016/j.jhazmat.2005.11.055.

Cruz, A.F.D., Norena, N., Kaushik, A., Bhansali, S., 2014. A low-cost miniaturized potentiostat for point-of-care diagnosis. Biosens. Bioelectron. 62, 249–254. https://doi.org/10.1016/j.bios.2014.06.053.

Duffó, G.S., Farina, S.B., Giordano, C.M., 2010. Characterization of solid embeddable reference electrodes for corrosion monitoring in reinforced concrete structures. Mater. Corros. 61, 480–489. https://doi.org/10.1002/maco.200905346.

Fattori, V., Hohmann, M., Rossaneis, A., Pinho-Ribeiro, F., Verri, W., 2016. Capsaicin: current understanding of its mechanisms and therapy of pain and other pre-clinical and clinical uses. Molecules 21, 844. https://doi.org/10.3390/molecules21070844.

Jin, M., Jiang, L., Xu, J., Chu, H., Tao, D., Bai, S., Jia, Y., 2016. Electrochemical characterization of solid Ag/AgCl reference electrode with different electrolytes for corrosion monitoring of steel in concrete. Electrochem. Soc. Jpn. 2, 383–389. https://doi.org/10.5796/electrochemistry.84.383.

Johanson Technology, 2012. Johanson Technology, Inc., Highly temperature-stable Impedance Matched RF Front End Differential Balun-Low Pass Filter Integrated Ceramic Component [WWW Document]. URL ⟨https://www.johansontechnology.com/2450bm15a0002-matched-balun-for-t-i-253x-family-chipsets⟩.

Kachoosangi, R.T., Wildgoose, G.G., Compton, R.G., 2008. Carbon nanotube-based electrochemical sensors for quantifying the "heat" of chilli peppers: the adsorptive stripping voltammetric determination of capsaicin. Analyst 133, 888. https://doi.org/10.1039/b803588a.

Kutluay, A., Aslanoglu, M., 2017. Sensitive determination of capsaicin in pepper samples using a voltammetric platform based on carbon nanotubes and ruthenium nanoparticles. Food Chem. 228, 152–157. https://doi.org/10.1016/j.foodchem.2017.01.161.

Lau, B.B.Y., Panchompoo, J., Aldous, L., 2014. Extraction and electrochemical detection of capsaicin and ascorbic acid from fresh chilli using ionic liquids. New J. Chem. https://doi.org/10.1039/C4NJ01416B.

Manaia, M.A.N., Diculescu, V.C., Gil, E.D.S., Oliveira-Brett, A.M., 2012. Guaicolic spices curcumin and capsaicin electrochemical oxidation behaviour at a glassy carbon electrode. J. Electroanal. Chem. 682, 83–89. https://doi.org/10.1016/j.jelechem.2012.06.023.

McIlhenny Company, 2018. Scoville Chart [WWW Document]. URL 〈https://www.tabasco.com/product/chipotle-sauce/〉 (Accessed 8 August 2018).

Mohammad, R., Ahmad, M., Heng, L.Y., 2013. An amperometric biosensor utilizing a ferrocene-mediated horseradish peroxidase reaction for the determination of capsaicin (chili hotness). Sensors (Switz.) 13, 10014–10026. https://doi.org/10.3390/s130810014.

Mohammad, R., Ahmad, M., Heng, L.Y., 2017. Amperometric capsaicin biosensor based on covalent immobilization of horseradish peroxidase (HRP) on acrylic microspheres for chilli hotness determination. Sens. Actuators B Chem. 241, 174–181. https://doi.org/10.1016/j.snb.2016.10.077.

Mpanza, T., Sabela, M.I., Mathenjwa, S.S., Kanchi, S., Bisetty, K., 2014. Electrochemical determination of capsaicin and silymarin using a glassy carbon electrode modified by gold nanoparticle decorated mulitiwalled carbon nanotubes. Sensors 2813–2828. https://doi.org/10.1080/00032719.2014.924010.

Randviir, E.P., Metters, J.P., Stainton, J., Banks, C.E., 2013a. Electrochemical impedance spectroscopy versus cyclic voltammetry for the electroanalytical sensing of capsaicin utilising screen printed carbon nanotube electrodes. Analyst. https://doi.org/10.1039/c3an00368j.

Randviir, E.P., Metters, J.P., Stainton, J., Banks, C.E., 2013b. Electrochemical impedance spectroscopy versus cyclic voltammetry for the electroanalytical sensing of capsaicin utilising screen printed carbon nanotube electrodes. Analyst 138, 2970. https://doi.org/10.1039/c3an00368j.

Ruas de Souza, A.P., Bertotti, M., Foster, C.W., Banks, C.E., 2015. back-to-back screen-printed electroanalytical sensors: extending the potential applications of the simplistic design. Electroanalysis 27, 2295–2301. https://doi.org/10.1002/elan.201500155.

Satyanarayana, M.N., 2006. Capsaicin and gastric ulcers. Crit. Rev. Food Sci. Nutr. 46, 275–328. https://doi.org/10.1080/1040-830491379236.

Scoville, W., 1912. Note on capsicum. Am. Pharm. Assoc. 1, 453–454. https://doi.org/10.1002/jps.3080010520.

Singh, A., 2013. Gas Sensor Platform Reference Design.

Turner, A.P.F., 2013. Biosensors: sense and sensibility. Chem. Soc. Rev. 42, 3184. https://doi.org/10.1039/c3cs35528d.

Wang, J., 2001. Glucose biosensors: 40 Years of advances and challenges. Electroanalysis 13, 983–988. https://doi.org/10.1002/1521-4109(200108)13:12<983::AID-ELAN983>3.0.CO;2-#.

Wang, Y., Huang, B., Dai, W., Ye, J., Xu, B., 2016. Sensitive determination of capsaicin on Ag/Ag2O nanoparticles / reduced graphene oxide modified screen-printed electrode. JEAC 776, 93–100. https://doi.org/10.1016/j.jelechem.2016.06.031.

Ya, Y., Mo, L., Wang, T., Fan, Y., Liao, J., Chen, Z., Manoj, K.S., Fang, F., Li, C., Liang, J., 2012a. Highly sensitive determination of capsaicin using a carbon paste electrode modified with amino-functionalized mesoporous silica. Colloids Surf. B Biointerfaces 95, 90–95. https://doi.org/10.1016/j.colsurfb.2012.02.025.

Ya, Y., Mo, L., Wang, T., Fan, Y., Liao, J., Chen, Z., Srivastava, K., Fang, F., Li, C., Liang, J., 2012b. Highly sensitive determination of capsaicin using a carbon paste electrode modified with amino-functionalized mesoporous silica. Colloids Surf. B Biointerfaces 95, 90–95. https://doi.org/10.1016/j.colsurfb.2012.02.025.

Yard, Y., Zühre, Ş., 2013. Electrochemical evaluation and adsorptive stripping voltammetric determination of capsaicin or dihydrocapsaicin on a disposable pencil graphite electrode. Talanta 112, 11–19. https://doi.org/10.1016/j.talanta.2013.03.047.

Yardım, Y., 2011. Sensitive detection of capsaicin by adsorptive stripping voltammetry at a boron-doped diamond electrode in the presence of sodium dodecylsulfate. Electroanalysis.